

Seismic fragility curves for damage to building contents

Haider A. Al Abadi, Nelson T.K. Lam and Emad F. Gad

Abstract

Slender free-standing objects in a building could be excited into rigorous rocking and/or sliding motion in an earthquake. Some objects might experience overturning and hence damage when impacting on the floor. Objects which do not overturn might still experience significant damage depending on the severity and nature of the collision with the neighbouring objects and with the floor when excited into motion. This paper presents fragility curves which define the probability of overturning of objects for given object dimensions, dynamic characteristics of the building and location of the object within the building. A method for calculating the level of shock experienced by the object on pounding with the floor is also presented.

1. Introduction

Contemporary codes of practice typically relate the seismic actions on non-structural components and building contents to the maximum acceleration of the floor (eg. Draft AS 1170.4, 2006; AS/NZS 1170.5, 2005). A dynamic amplification factor may be applied depending on whether the component is attached to a flexible mounting. This method of analysis does not accurately take into account the highly non-linear behaviour of the rocking motion in which overturning would occur if the centre of gravity of the object has been displaced past the pivotal position of rocking. For objects that have not overturned, significant level of damage might still be caused by the pounding of the object with the floor and with neighbouring objects. The research described in this paper is aimed at modelling the vulnerability of objects to overturning. Results are presented in the form of fragility (vulnerability) curves in Section 2. A simple method of estimating shock sustained by objects which do not overturn will also be described in Section 3.

2. Vulnerability of objects to overturning

Fragility curves are normally presented to predict the probability of damage to a structure, or component, with increasing intensity of the applied actions. With seismic actions, the intensity is usually represented by the notional peak ground acceleration (PGA), or peak ground velocity (PGV). Similar fragility curves could be used to predict the extent of damage to non-structural components in a building. However, this conventional format of presenting vulnerability to damage is not as effective in providing information on the relative vulnerability for a range of components with different properties, since only one item of interest is represented by each curve. Fragility curves for overturning of objects as presented in this paper are mostly based on correlating the probability of overturning with variations in object height when the thickness and shape of the object is kept constant (eg. Figure 1). Fragility diagrams presented later in the paper contain multiple fragility curves with each representing objects of a constant thickness but varying height (eg. Figure 2a). Thus, the relative vulnerability to overturning can be shown for objects of varying size and aspect ratio in one diagram.

In this study, the earthquake excitations were based on an ensemble of six artificial accelerograms with random phase-angles generated by program GENQKE (Lam et al, 2000) to simulate the ground shaking of a Class D site in a magnitude 6.5 earthquake at a site-source distance of 45 km. The attenuation of the earthquake with distance was based on the crustal model of south-eastern Australia as adopted in the study of Lam et al (2005). The intensity and frequency content of the simulated motions were consistent with the design response spectrum stipulated by the new Australian Standard for seismic actions for a seismic coefficient of $Z = 0.08$, which is the level of seismic hazard defined for most Australian capital cities on the eastern seaboard including Melbourne, Sydney and Canberra for a return period of 500 years (Draft AS1170.4, 2006).

The objective at this stage of the investigation was to reveal the trend of the vulnerability to overturning. Hence, only one earthquake scenario was considered. Uncertainties associated with the buildings' dynamic properties and objects' dimensions have not been incorporated into the fragility curves, in which the random variability of the applied excitations was only taken into account. These fragility curves can be further developed to incorporate variability in the objects' dimensions and other related parameters.

All the rectangular objects were assumed to be free-standing, resting on a perfectly inelastic surface, and have uniform distribution of mass. The filtering of the floor motions was in accordance with: (i) the fundamental mode of vibration of a ten-storey building with natural period equal to 1 second and a linear deflection profile, and (ii) the first three modes of vibration of a 66-storey building model of height 280 m based on micro-tremor monitoring of the Republican Plaza, Singapore (Brownjohn & Pan, 2001). The fundamental natural period of vibration of the second building model was 5.4 seconds.

When the object thickness (t) was fixed, non-linear time-history analyses that could simulate large displacement (rocking) behaviour were applied to objects with heights varying between $h = 0.1$ m to 4 m (with 100 mm increments) to determine if the object could overturn. Details of this type of analyses have been presented in Al Abadi et al, 2004 & 2006. The total number of simulations in the construction of a fragility curve was 240 (ie. 6 accelerograms x 40 models of varying height). An example of such a fragility curve is shown in Figure 1 in which the object thickness was kept at $t = 100$ mm and the floor excitations were subject to filtering of the 10-storey building up at the roof level. The scattered plot shown by the "diamond" symbols in the figure indicate the actual percentage of overturning observed from the 6 analyses undertaken for every increment of object height h . The solid line shown in the figure represents the "best-fit" cumulative log-normal probability density function $F\{h\}$ which is parameterized by the mean and standard deviation of h (with notation m and s respectively) as shown by equation (1). Statistical analyses have been applied to verify the adopted function form for the fragility curves and to test the "goodness-of-fit" (Shinozuka et al, 2001). It is noted that 240 models were analysed for each object thickness in order that a reliable estimation of the mean and log-standard deviation could be achieved.

The "optimal" values of m and s that achieve the best match of the $F\{h\}$ function with the observed rate of overturning were calculated using the Maximum Likelihood Theory (Shinozuka et al, 2000) which is briefly described herein. With overturning analyses undertaken on 240 cases (ie. $N = 240$) the maximum likelihood parameter L is defined by equation (2).

$$F\{h\} = \Phi\left\{\frac{\ln(h/\mu)}{\sigma}\right\} \quad (1)$$

$$L = \prod_{i=1}^N (F\{h_i\})^{x_i} (1 - F\{h_i\})^{1-x_i} \quad (2)$$

where i identifies each of the N ($=240$) no. of cases and $x_i = 1$ or 0 if overturning is predicted to occur, or not to occur, respectively by the time-history analysis. The values of μ and σ were determined for the conditions where the value of L as defined by equation (2) was maximized, using equations (3a) and (3b) respectively.

$$\frac{\partial \ln(L)}{\partial \mu} = 0 \quad (3a)$$

$$\frac{\partial \ln(L)}{\partial \sigma} = 0 \quad (3b)$$

Figure 1 provides a holistic, and simple, representation of vulnerability of objects to overturning with $t = 100$ mm and floor excitations as specified. It is shown that with such conditions most objects of height equal to, or exceeding 1 m, would be most likely to overturn (with probability of overturning close to 100 %). The probability is reduced to slightly above 50% for object height equal to half a metre.

Further fragility curves were constructed for different object thicknesses and excitations based on different floor levels within the 10-storey and the 66-storey buildings (refer fragility curves presented in Figure 2).

It is shown that the fragility curves are very sensitive to the object thickness. For example, the probability of overturning of objects with thickness equal to 500 mm never exceeds 50 %. The floor level within the building and the nature of the building could both be very critical to the object overturning behaviour (Franke et al, 2005). For example, objects in the 66-storey building are much less likely to overturn than in the 10-storey building when other parameters are kept the same. Objects positioned at mid-height of the 66-storey building appear least vulnerable out of all the presented cases.

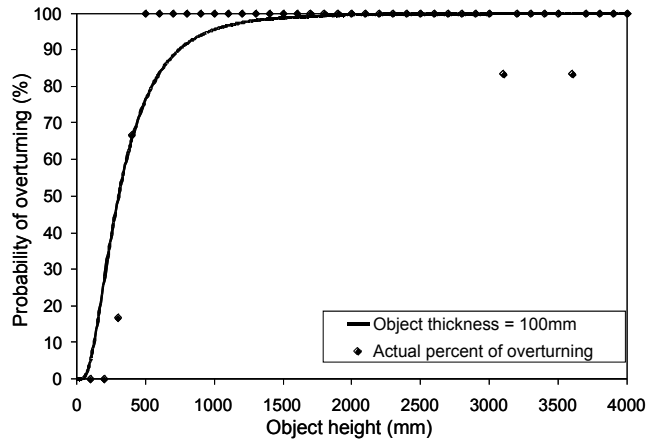
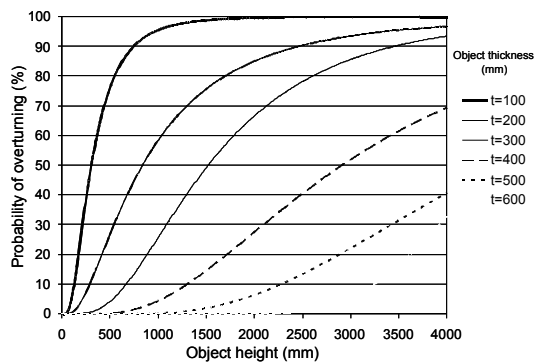
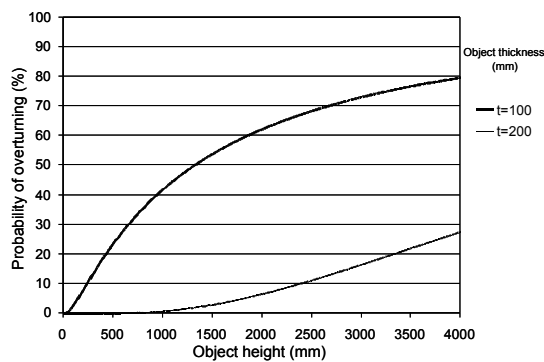


Figure 1: Fragility curve for 100mm thick objects at roof of 10-storey building

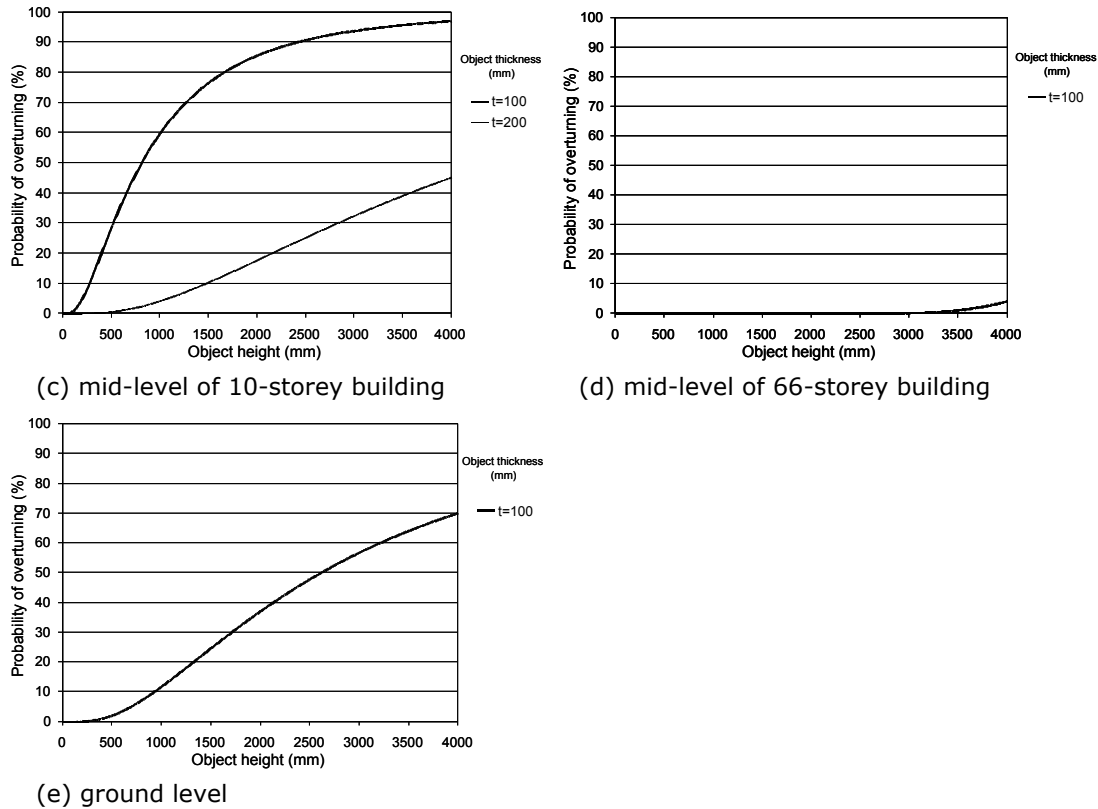
Fragility curves can also be extended to incorporate multiple earthquake scenarios that have been identified from the de-convolution analysis of the seismic hazard model for an area (in which case vulnerability curves associated with any pre-defined level of PGV could be obtained by aggregating probability of overturning calculated for each contributing earthquake scenario; refer companion paper Lumantarna et al, 2006). Example of such fragility curves is shown in Figure 3 for specific objects of certain dimensions.



(a) Roof of 10-storey building



(b) Roof of 66-storey building



Figures 2: (a) – (e) Fragility curves at different levels within 10-storey and 66-storey buildings

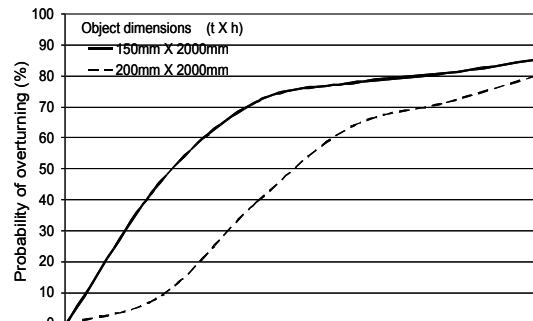


Figure 3: Fragility curves at the rooftop of 10-storey building for two rectangular objects

3. Modeling level of shock on rocking objects

Objects that do not overturn might still be damaged (or have their contents damaged) by shocks sustained at the base of the object when pounding on the floor during the course of rocking. In the worst case (ie. at the threshold of overturning) the centre of gravity (c.g.) of the rectangular object could be displaced by an amount equal to half of the object thickness (ie. $t/2$). The angle of rotation of a slender object measured from the horizontal is accordingly equal to t/h and its c.g. lifted by the amount defined by equation (4).

The potential energy gained by the lifting of the object as defined by equation (5) will all be converted to kinetic energy which would in turn be dissipated by the impact (it is assumed that the base of the object would not fall flat on the floor but instead only its edge is engaged with the impacting action).

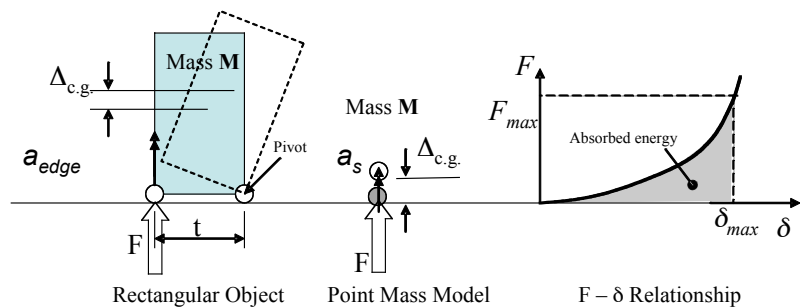
$$\Delta_{c.g.} = \frac{t^2}{2h} \tag{4}$$

$$PE = M \cdot g \cdot \Delta_{c.g.} = \frac{M \cdot g \cdot t^2}{2h} \tag{5}$$

It is the objective of this section to describe the modeling that is required to predict the level of shock experienced on impact. Factors controlling the impacting actions include the amount of kinetic energy to be dissipated, the geometry and stiffness properties of the object, and the stiffness property of the flooring materials and details of the edge of the object which is engaged with the impact. Modeling the impacting action by finite elements may consume a great deal of memory since very fine meshing is required of both the object and the floor surrounding the point of impact. Significantly, the time-step has to be very small given that the impact would only last for a few milliseconds depending on the hardness of the materials that are affected. Given that the computations need to take into account geometrical non-linearity, the dynamic stiffness matrix requires reconstruction at every time-step. Thus, the amount of computational time increases exponentially with the number of degrees of freedom in the finite element model.

The investigation described herein was concerned with a computer server cabinet (which can be modeled as a rectangular body). Small studs were attached to the edges of the cabinet at the base. Thus, the floor surface was in direct contact with the surface of the studs as illustrated in Figure 4. An important feature of the modeling was the simplification of the cabinet into a point mass object model. The size and geometry of the object was to match with that of the studs but the density of the point mass was artificially increased in order that its total mass (M) was made to equate with that of the cabinet as a whole. If the point mass was lifted by the amount defined by equation (4) the potential energy gained by the lifting would then be identical to the potential energy gained by the lifting of the cabinet as defined by equation (5). Given that the force-indentation relationship, or $F\{\delta\}$, of the base stud of the cabinet into the flooring material has been accurately represented by the point mass model, the force (F) experienced by the floor would also be accurately represented at any instance during the impact.

Figure 4 Rectangular object model and point mass object model



Finite element analysis could be undertaken on the point mass object impacting on the floor for calculating the level of shock ($a_s = F/M$). This approach to modeling waives the need to model the cabinet as finite elements and hence represents significant savings in computational time. If the stud was spherical, the analysis could be simplified further by employing closed-form solutions (Hertz law) to model the force-indentation relationship of a sphere impacting on the floor (which is modelled as a half-space). In fact, the point mass model could take any geometry which matches with the actual shape of the stud. For example, the geometry of the point mass can take the shape of the rubber stud commonly used for isolating the base of metal cabinets from the floor. If the floor surface was an order of magnitude harder than that of the stud, the force-indentation, or $F\{\delta\}$, relationship could be based purely on the stiffness behaviour of the stud in isolation, in

which case no finite element modeling would be required. No matter which approach is used to obtain the $F - \delta$ curve, the maximum impact force (F_{\max}), and maximum indentation (δ_{\max}), could be identified at the point on the curve where the total amount of absorbed energy equals the amount of potential energy defined by equation (5). This method of calculating the value of F_{\max} , and hence $a_{s \max}$ ($= F_{\max}/M$) is summarized by equations (6a) – (6b).

$$\frac{M \cdot g \cdot t^2}{2h} = \int_{\delta=0}^{\delta_{\max}} F\{\delta\} d\delta \quad (6a)$$

$$a_{s \max} = \frac{F\{\delta_{\max}\}}{M} \quad (6b)$$

Equations (6a) and (6b) were based on the worst case of an object being lifted to the limit of overturning. These equations could be modified for calculating the value of $a_{s \max}$ for any arbitrary lift of the object.

Finally, the level of shock experienced by the cabinet at its edge (a_{edge}) can be related to the calculated value of $a_{s \max}$ using equations (6c) – (6d) which were derived by taking moment about the pivotal edge of rocking, and by equating the calculated moment to the rate of change of angular momentum immediately following impact.

$$F_{\max} \cdot t = I_o \cdot \ddot{\theta} = \frac{4}{3} MR^2 \frac{a_{\text{edge}}}{t} \quad (6c)$$

$$a_{\text{edge}} = \frac{3t^2}{4MR^2} a_{s \max} \quad (6d),$$

where R is the length measured from the centre of the object to its corner, I_o is the mass moment of inertia of the cabinet around the pivotal edge ($I_o = 4/3 M_b R^2$), and $\ddot{\theta}$ is the angular acceleration of the object during impact ($\ddot{\theta} = a_{\text{edge}}/t$).

Equation (6d) is based on the assumption that the rocking motion of the rectangular object comes to an abrupt end following the impact of the base stud with the floor. This assumption is generally valid for squat objects but may over-predict the amount of absorbed energy with slender objects. A more accurate expression to predict the value of a_{edge} is defined by equations (6e) – (6f) which takes into account the fact that only part of the kinetic energy is absorbed by the floor (and base stud) as the rocking motion continues due to the angular motion of the object.

$$a_{\text{edge}} = \frac{3t^2}{4MR^2} \cdot \frac{1}{\sqrt{1 - R_D^2}} a_{s \max} \quad (6e)$$

$$R_D = 1 - 0.375 \left(\frac{t}{R} \right)^2 \quad (6f)$$

where R_D is the ratio of the angular velocity immediately after and before the impact.

The accuracy of equations (6a) – (6f) in predicting the level of shock experienced by the edge of the cabinet (a_{edge}) has been evaluated experimentally by comparing the calculated values with the directly measured values (refer Table 1).

Table 1 Comparison of calculated and directly measured values of a_{edge}

Sample no.	$a_{s \max}$	a_{edge} from equations (6e) – (6f)	a_{edge} from direct measurements
1	7.3	3.3	3.4
2	7.3	3.3	3.45
3	10.4	4.6	4.9
4	10.4	4.6	4.8
5	11.5	5.1	5.3

4. Conclusions

This paper presents unique fragility curves for overturning of objects in buildings when subject to code-compatible earthquakes. These curves predict the probability of overturning for objects with different thicknesses and heights that are located at different levels with two example buildings. In addition, Fragility curves incorporating multiple earthquake scenarios that have been identified from the de-convolution analysis of the seismic hazard model for an area are also presented. Based on these curves critical objects as well as critical building levels can be easily identified. The paper also presents a methodology for estimating the maximum impact shock on objects due to rocking. An equivalent point mass system is proposed to represent solid rectangular objects to simplify the computation's time demand. This method would assist building owners and operators in ensuring continuing operation of critical components after an earthquake event.

References

- Al Abadi H., Lam N.T.K., and Gad E. (2006), "A Simple Displacement-Based Model for Predicting Seismically Induced Overturning", *Journal of Earthquake Engineering*, [Accepted].
- Al Abadi, H., Lam N.T.K., Gad E., and Chandler A.M. (2004), "Modelling of Earthquake Induced Overturning of Building Contents", *Proceedings of the Australian Earthquake Engineering Society Annual Technical Conference*. Mt. Gambier, South Australia, Australia, 5 – 7 October, 2004. Published by AEES. Paper no. 10.
- AS/NZS 1170.5 (2004). *Standard New Zealand, Structural design actions, Part 5: Earthquake actions*. New Zealand Commentary.
- Brownjohn J.M.W. and Pan T.C. (2001), "Response of tall buildings to weak long distance earthquakes", *Earthquake Engineering & Structural Dynamics*, 30(5):709-729.
- Draft AS/NZS 1170.4 - 2006. *Draft Australian Standard for Structural Design Actions, Part 4: Earthquake Actions in Australia*. Document No. D5212-5.1.
- Franke D, Lam N.T.K., Gad E., and Chandler A.M (2005), "Seismically Induced Overturning of Objects and Filtering Effects of Buildings", *Journal of Seismology and Earthquake Engineering*, 7 (2): 95-108.
- Lam, N.T.K., Wilson, J.L., and Hutchinson, G.L. (2000), "Generation of Synthetic Earthquake Accelerograms Using Seismological Modeling : A Review ", *Journal of Earthquake Engineering*, 4(3), 321-354.
- Lam, N.T.K., Wilson, J.L., and Venkatesan, S. (2005), "Accelerograms for dynamic analysis under the New Australian Standard for Earthquake Actions", *Electronic Journal of Structural Engineering*. 5: 10-35.
- Lumantarna, E., Vaculik, J., Griffith, M., Lam, N.T.K., and Wilson J.L. (2006), "Seismic Fragility Curves for Unreinforced Masonry Walls", *Proceedings of the Australian Earthquake Engineering Society Annual Technical Conference*, Canberra.
- Shinozuka, M., Feng, M. Q., Kim, H., Uzawa, T., Ueda, T. (2001), "Statistical Analysis of Fragility Curves", *Technical REspot MCEER, Department of Civil and Environmental Engineering, University of Southern California, Task Number 106-E-7.3.5 and 106-E-7.6*.
- Shinozuka, M., Feng, M. Q., Lee, J. H. and Nagaruma, T. (2000), "Statistical Analysis of Fragility Curves", *Proceeding of the Asian-Pacific Symposium on Structural Reliability*.

